

uncertainty as to the nature of the HOONO transition state, we make no attempt to interpret (21) quantitatively. However, note that no threshold energy terms appear in (21) which is due in part to the assumption that there is no barrier to association. Our results at 850 Torr are within the falloff region for the HONO₂ channel, and thus we might expect that these conditions would be more favorable for observing the less stable isomer.

Conclusions

We were unable to directly observe any HOONO as a product of reaction 1 using long-path absorption spectroscopy. From this we conclude that one or more of the following is true: that HOONO is not formed in significant quantities ($\leq 10\%$); that HOONO has only very weak infrared absorption in the region searched (1850–3850 cm⁻¹); or that the HOONO product is short lived due to reaction with NO₂, to isomerization to nitric acid on the reactor wall or in the gas phase, or to dissociation to reactants. Atkinson et al.⁴⁸ have reported *n*-alkyl nitrate, RONO₂, products from the reactions of *n*-alkyl peroxy radicals, RO₂, with NO. The reactions presumably proceed through the isomerization of an energetic peroxy nitrite intermediate: ROO + NO → [ROONO* ⇌ RONO₂*] → RONO₂. Their observations may be evidence for a similar rearrangement in the [HOONO*] adduct. The studies of Niki et al.¹⁴ and Leu¹⁵ indicate that the presence of excess NO₂ does not cause ClONO to isomerize to the more stable ClNO₂. Also the isomerization of ClONO in the gas phase and on reactor surfaces is reported to be very slow^{14,15,49,50} compared

to the time scale of our experiments. We conclude that the yield of HOONO is probably $\leq 10\%$ and therefore is not significant in the atmosphere.

We have shown that HONO₂ is the major product of reaction 1. From direct measurements under a wide variety of conditions the yield of HONO₂ accounts for between 65% and 100% of the reaction products.

Although there is little experimental information on the stability and structure of the HOONO isomer, several independent estimates of the HO–ONO bond dissociation energy indicate a value in the range 15 to 25 kcal mol⁻¹ is likely. Our unimolecular dissociation rate calculations predict a relatively low yield of HOONO, $\leq 20\%$ for this species. These calculations are consistent with our observations.

Further studies which would improve our knowledge of reaction 1 include product searches at longer IR wavelengths and in the near-UV. Also since HONO₂ is known to photolyze to produce OH and NO₂ in the near-UV, the photolysis of HONO₂ in an inert cyrogenic matrix should allow the radicals to recombine as HOONO within the host cage. It is possible that spectroscopic information on HOONO could be gained in a matrix experiment.

Acknowledgment. This work was supported in part by NOAA as part of the National Acid Precipitation Assessment Program, by the Chemical Manufacturers Association Technical Panel on Fluorocarbon Research, and by the National Aeronautics and Space Administration Upper Atmosphere and Space Services Program.

(48) Atkinson, R.; Carter, W. P. L.; Winer, A. M. *J. Phys. Chem.* **1983**, *87*, 2012.

(49) Molina, L. T.; Molina, M. J. *Geophys. Res. Lett.* **1977**, *4*, 83.

(50) Janowski, B.; Knauth, H. D.; Martin, H. *Ber. Bunsen-Ges. Phys. Chem.* **1977**, *81*, 1262.

Kinetics of the High Temperature Reaction of CO with N₂O

Nobuyuki Fujii, Tomohisa Kakuda, Nobuhiro Takeishi, and Hajime Miyama*

Department of Chemistry, The Technological University of Nagaoka, Kamitomioka, Nagaoka, Niigata, 940-21, Japan (Received: July 23, 1986)

Kinetics of the high temperature reaction of CO with N₂O was investigated in a shock tube. For CO₂ formation in CO–N₂O–He–Ar mixtures, it was found that the bimolecular reaction (1) CO + N₂O → CO₂ + N₂ was predominant below 2000 K and the termolecular recombination (6) CO + O + M → CO₂ + M became important above 2000 K. The rate constants of the reactions were determined by a comparison of the calculated infrared emission profiles of CO₂ with those observed by experiments. The rate constants were found to be $k_1 = 9.8 \times 10^{10} \exp(-73 \text{ kJ}/RT) \text{ cm}^3 \cdot \text{mol}^{-1} \cdot \text{s}^{-1}$ and $k_6 = 1.6 \times 10^{15} \exp(-30 \text{ kJ}/RT) \text{ cm}^6 \cdot \text{mol}^{-2} \cdot \text{s}^{-1}$.

Introduction

Recently, the oxidation of CO with N₂O at high temperatures has received much attention as a possible system for a CO₂ gas dynamic laser.¹ Shock-heated CO + N₂O diluted with inert gas was forced to expand through a nozzle, where a higher value of small signal gain was obtained compared with the conventional CO₂ + N₂ system.²⁻⁴ In order to confirm whether this high gain is due to the reaction between CO and N₂O, it is necessary to clarify the reaction in the shock wave and the expansion flow. As the first step, the reaction kinetics of the CO + N₂O system at

TABLE I: Reaction Scheme and Rate Parameters^a

reaction	log A	B	E/kJ	ref
(1) N ₂ O + CO = N ₂ + CO ₂	10.99	0	73.0	this work
(2) N ₂ O + M = N ₂ + O + M	15.21	0	257.7	16
(3) N ₂ O + O = N ₂ + O ₂	14.00	0	117.2	14
(4) N ₂ O + O = NO + NO	13.84	0	111.3	14
(5) NO ₂ + O = NO + O ₂	13.30	0	4.6	7
(6) CO + O + M = CO ₂ + M	15.20	0	30.0	this work
(7) NO + O + M = NO ₂ + M	14.95	0	-7.5	7

^a $k = AT^B \exp(-E/RT)$ (in units of cm³·mol⁻¹ and s⁻¹).

high temperatures was examined in this study.

It has been generally considered that the reaction of CO with N₂O proceeds via two channels (see Table I): (1) the highly exothermic bimolecular reaction CO + N₂O → CO₂ + N₂, and (2) a set of reactions initiated by the dissociation of N₂O.⁵

(5) Loirat, H.; Caralp, F.; Destrian, M. *J. Phys. Chem.* **1983**, *87*, 2455.

(1) Kudryavtsev, N. N.; Kryuchkov, S. I.; Novikov, S. S.; Shcheglov, V. N.; Soloukhin, R. I. *Fifth Gas Flow and Chemical Lasers Symposium*; Adam Hilger Ltd.: Bristol, 1984; p 425.

(2) Kudryavtsev, N. N.; Novikov, S. S.; Svetlichnyi, I. B. *Sov. Phys. Dokl.* **1975**, *19*, 831.

(3) Kudryavtsev, N. N.; Novikov, S. S.; Svetlichnyi, I. B. *Sov. Phys. Dokl.* **1976**, *21*, 748.

(4) Kovtun, U. U.; Kudryavtsev, N. N.; Novikov, S. S.; Svetlichnyi, I. B.; Shagov, P. N. *Sov. Phys. Dokl.* **1978**, *23*, 503.

Especially the former reaction plays an important role below about 2000 K. However, the latter reactions became important above 2000 K because of the high activation energy for the dissociation of N₂O.

High temperature measurements of the rate constant for the bimolecular reaction have been performed by several researchers:⁵⁻⁸ Lin and Bauer⁶ and Milks and Matula,⁷ measured the rate constant by the single-pulse shock tube method. Zaslanko et al.⁸ determined the rate constant by measuring the ultraviolet absorption of N₂O and the luminescence due to the O + CO recombination for N₂O diluted with Ar or CO. Also, Loirat et al.⁵ obtained the rate constant from the measurement of the critical ignition pressure. However, there is a large discrepancy among the reported rate constants (see Figure 4).

The rate constant for the termolecular recombination (6) CO + O + M → CO₂ + M at high temperature has also been measured by several researchers.^{6,8,9} Lin and Bauer⁶ measured k_6 together with k_1 and reported the value of k_6 with a negative activation energy. Also, Zaslanko et al.⁸ measured k_6 together with k_1 . Dean and Steiner⁹ obtained a lower value for k_6 by measuring 4.27- μ m and 450-nm emission for shock-heated CO-N₂O-Ar mixtures in the temperature range 2100-3200 K (see Figure 5).

Previously, the authors¹⁰ investigated the reaction system by measuring the infrared emission of CO₂ produced behind reflected shock waves and reported preliminary results for the values of k_1 and k_6 . Later, they found that impurities of He (99.9%) had a serious effect on the rate measurement. Therefore, in the present study, the same experiment was repeated more carefully by using He of high purity (99.9995%).

Experimental Section

The experiments were carried out in a 78-mm stainless steel shock tube, consisting of a 3.5-m-long test section and a 1.5-m-long high-pressure section. The shock tube had a leak rate of less than 2×10^{-3} Torr·min⁻¹ and was evacuated to less than 1×10^{-3} Torr by using an oil-diffusion pump with a water-cooled baffle and a liquid N₂ cold trap. Here, the oil back streaming rate was $<10^{-8}$ mg·cm⁻²·min⁻¹. The incident shock wave velocity was measured by four piezoelectric gauges located at intervals of 300 mm and a time counter. Temperature (T_{50}) and pressure (p_{50}) behind the reflected shockwave were calculated from the incident shock velocity by the conventional method.¹¹ Typical errors in the temperature measurement were within 20 K. An observation window of CaF₂ and a piezoelectric pressure gauge were set at 35 mm from the end plate of the shock tube.

The time history of CO or CO₂ was monitored by measuring the infrared emission isolated with an interference filter (4.87 μ m with fwhm = 0.24 μ m for CO and 4.25 μ m with fwhm = 0.16 μ m for CO₂). The temperature dependence of the CO₂ emission intensity at 4.25 μ m was measured by using shock-heated CO₂-Ar mixtures. Also that of N₂O emission intensity at 4.25 μ m was measured independently by using shock-heated N₂O-Ar mixtures, because the emission of N₂O was observed through the 4.25- μ m filter. The emission intensity of N₂O was about a tenth of that of CO₂. The emission signal obtained from a liquid-nitrogen-cooled InSb detector and the pressure signal were displayed on a digital storage oscilloscope.

Experiments were carried out on mixtures of CO and N₂O diluted with He and Ar (CO/N₂O/Ar/He = 2-5/2-5/46-40/50), which were heated behind the reflected shock waves in the temperature range of 1400-2500 K and at a pressure of about 3.0 atm. Here, He was added to reduce the vibrational relaxation

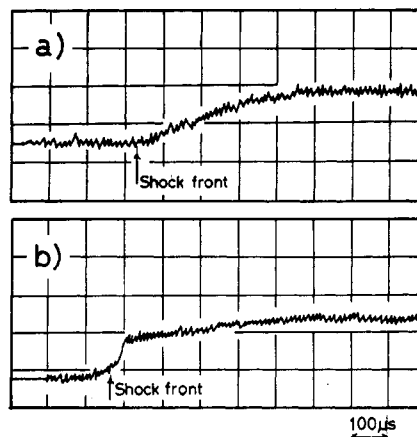


Figure 1. Typical oscillogram of 4.87- μ m infrared emission: (a) CO/Ar = 1/99, $T_0 = 1842$ K, $p_0 = 2.42$ atm; (b) CO/Ar/He = 1/49/50, $T_0 = 1885$ K, $p_0 = 2.42$ atm.

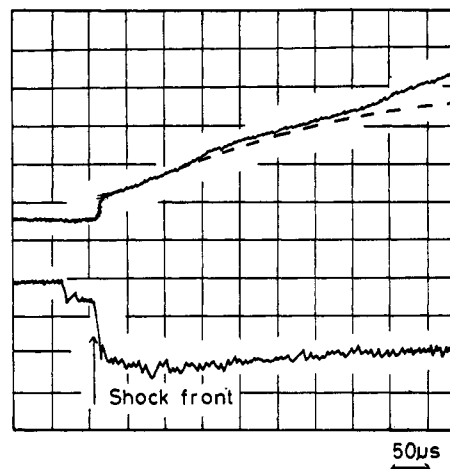


Figure 2. Typical oscillogram of 4.25- μ m infrared emission (upper trace) and or pressure (lower trace). Mixture A, $T_0 = 2484$ K, $p_0 = 3.35$ atm.

time of CO. The gases used in the experiments were obtained from commercial suppliers and the purities of the gases were as follows: CO, 99.9% (O₂ < 100 ppm, H₂O < 15 ppm); N₂O, 99.9% or 98% (O₂ < 1.4%, N₂ < 0.6%, 600 ppm); Ar, 99.998%; He, 99.9995%. N₂O was purified by the trap-to-trap method using dry ice and liquid N₂ and the other gases were used without further purification.

Results and Discussion

The vibrational relaxation of CO in CO-Ar and CO-CO systems is known to be very slow.¹² Then, as a preliminary experiment, the relaxation time was observed by measuring the CO infrared emission at 4.87 μ m on mixtures of CO/Ar = 1/99 and CO/Ar/He = 1/49/50. Examples of CO emission are shown in Figure 1. From the figure, it was found that the relaxation time of CO for the former mixture was about 300 μ s at $T_0 = 1840$ K and $P_0 = 2.4$ atm, and the time for the latter mixture was about 20 μ s at $T_0 = 1885$ K and $P_0 = 2.4$ atm. Accordingly, in order to reduce the effect of the vibrational relaxation time of CO on the rate measurement, He was added to Ar as a diluent (He, 50%) in all of the following experiments.

A typical profile for the 4.25- μ m emission on a mixture of CO-N₂O-Ar-He behind the reflected shock wave is shown in Figure 2. The initial rise of the emission is due to shock-heated N₂O, and the subsequent linear rise is due to CO₂ production. The slope of the linear rise was found to be nearly proportional to the initial concentration of CO and N₂O, respectively. The emission profiles were compared with those obtained by a simulation, in which the concentrations of N₂O and CO₂ calculated

(6) Lin, M. C.; Bauer, S. H. *J. Chem. Phys.* **1969**, *50*, 3377.
 (7) Milks, D.; Matula, R. A. *Symp. (Int.) Combust. [Proc.]*, **14th** **1973**, 83.
 (8) Zaslanko, I. S.; Losev, A. S.; Mozhukhin, E. V.; Mukoseev, Yu. K. *Kinet. Katal.* **1979**, *20*, 1385. *Engl. Transl.* **1979**, *80*, 1144.
 (9) Dean, A. M.; Steiner, D. C. *J. Chem. Phys.* **1977**, *66*, 598.
 (10) Fujii, N.; Kakuda, T.; Sugiyama, T.; Miyama, H. *Chem. Phys. Lett.* **1985**, *122*, 489.
 (11) Gardiner, Jr., W. C. In *Shock Wave in Chemistry*, Lifshitz, A., Ed.; Marcel Dekker: New York, 1981; p 319.

(12) Millikan, R. C.; White, D. R. *J. Chem. Phys.* **1963**, *39*, 3209.

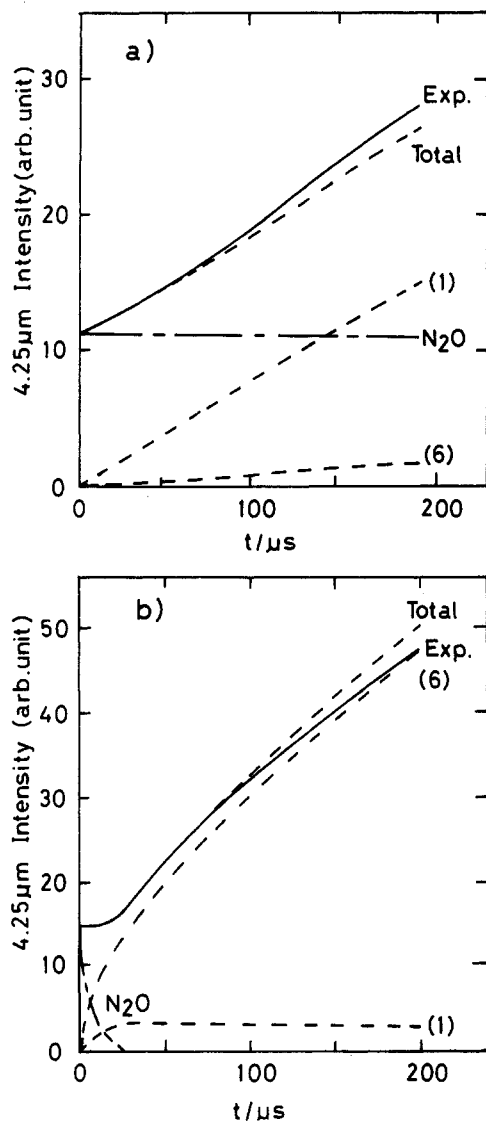


Figure 3. Comparison of the 4.25- μm emission profile with calculated profiles. Exp.: experimental emission intensity. Other lines are calculated values, (1) and (6) correspond to the emissions from CO_2 produced by reactions 1 and 6, respectively. N_2O : emission due to N_2O . Total: sum of the emission intensities from CO_2 and N_2O . (a) Mixture C, $T_0 = 1526$ K, $p_0 = 2.88$ atm. (b) Mixture A, $T_0 = 2484$ K, $p_0 = 3.35$ atm.

from the reaction scheme were converted into the emission intensity by using the calibration curves obtained from the shock-heated N_2O -Ar and CO_2 -Ar experiments. Here, the comparisons were performed in the initial stage of the reaction (within about 200 μs), in order to reduce the effects of subsequent reactions. Examples of the comparisons are shown in Figure 3, a and b.

The scheme of the high-temperature reaction of CO with N_2O used in the simulation is shown in Table I. Here, two channels are responsible for the formation of CO_2 : (1) a highly exothermic bimolecular reaction of CO and N_2O (reaction 1), and (2) a set of elementary reactions initiated by the dissociation of N_2O (reactions 2-7).⁵ In this calculation, differential equations for reactions 1-7 and their reverse reactions were solved numerically, coupled with a heat balance equation and gas flow equations for the reflected shock wave.¹¹

Below about 2000 K, CO_2 formation by reaction 6 was confirmed to be negligible under the present conditions because of the slow decomposition rate of N_2O . Accordingly, the rate constant k_1 of reaction 1 can be determined directly by a comparison of the profiles of 4.27- μm emission from the experiments with the calculated values using reaction 1 as shown in Figure 3a.

Above 2000 K, CO_2 formation by reaction 1 was almost terminated in the very early stage of reaction because of the fast

TABLE II: Experimental Conditions and Obtained Rate Constants

mixture	CO , %	N_2O , %	T_{50} , K	p_{50} , atm	k_1 , $\text{cm}^3\cdot\text{mol}^{-1}\cdot\text{s}^{-1}$	k_6 , $\text{cm}^6\cdot\text{mol}^{-2}\cdot\text{s}^{-1}$
A (●)	2	2	1568	2.78	3.82×10^8	
			1701	3.11	7.17×10^8	1.96×10^{14}
			1771	2.84	6.07×10^8	2.06×10^{14}
			1905	3.05	1.05×10^9	2.24×10^{14}
			2170	3.19	2.16×10^9	3.11×10^{14}
			2205	2.84	1.53×10^9	3.36×10^{14}
B (Δ)	4	2	2484	3.35	2.28×10^9	3.35×10^{14}
			1510	2.89	3.30×10^8	
			1533	2.74	3.92×10^8	
			1719	3.03	5.91×10^8	1.98×10^{14}
			1869	2.86	9.42×10^8	2.19×10^{14}
			1930	2.82	1.20×10^9	2.28×10^{14}
C (▲)	4	4	2406	3.29	3.46×10^9	3.66×10^{14}
			1424	2.93	2.14×10^8	
			1430	2.79	2.50×10^8	
			1519	2.99	2.78×10^8	
			1526	2.88	2.48×10^8	
			1725	3.28	4.64×10^8	1.99×10^{14}
			1808	3.75	6.10×10^8	2.11×10^{14}
			1887	2.89	8.04×10^8	2.22×10^{14}
			1966	3.07	9.55×10^8	2.33×10^{14}
			2048	2.78	1.43×10^9	2.43×10^{14}
D (○)	5	5	2307	2.33	3.00×10^9	3.52×10^{14}
			2482	2.21	3.06×10^9	3.76×10^{14}
			1458	2.99	2.83×10^8	
			1461	3.00	2.02×10^8	
			1492	2.93	2.33×10^8	
			1511	2.94	2.39×10^8	
			1757	3.45	5.66×10^8	2.40×10^{14}
			1950	2.42	8.92×10^8	2.30×10^{14}
			1989	3.12	1.04×10^9	3.02×10^{14}
			2378	2.43	1.98×10^9	3.62×10^{14}
2461	2.26	2.97×10^9	3.93×10^{14}			

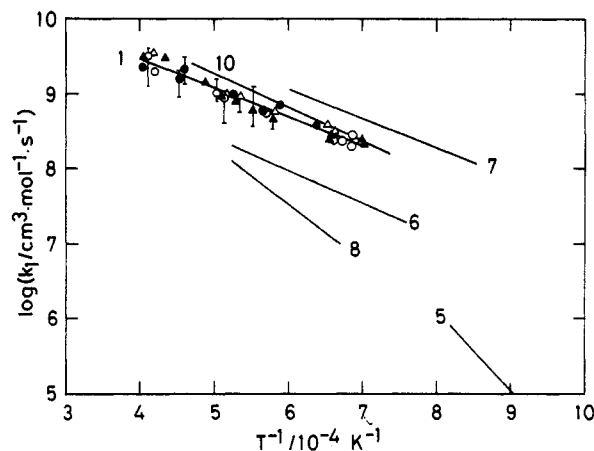


Figure 4. Arrhenius plots of the rate constants for $\text{CO} + \text{N}_2\text{O} \rightarrow \text{CO}_2 + \text{N}_2$: 1, this work (●, Δ, ▲, and ○ correspond to mixtures A, B, C, and D, respectively.); 6, in Lin et al.;⁶ 7, Milks et al.;⁷ 8, Zaslanko et al.;⁸ 5, Loirat et al.;⁵ 10, Fujii et al.¹⁰

consumption of N_2O , and CO_2 formation via the second channel became important as shown in Figure 3b. The high-temperature decomposition of N_2O has been studied by many researchers and its reaction scheme is well established.^{13,14} Since k_1 can be determined below 2000 K as described above, k_6 can be calculated from the CO_2 emission profile by using the extrapolated value of k_1 . Thus the rate constant k_6 was determined by comparison of the 4.25- μm emission profile with simulations.

The values of k_1 and k_6 were further corrected by comparison in the wide temperature range of 1400-2500 K. The rate constants

(13) Just, T. In *Shock Waves in Chemistry*, Lifshitz, A., Ed.; Marcel Dekker: New York, 1981; p 279.

(14) Hanson, R. K.; Salimian, S. In *Combustion Chemistry*, Gardiner, Jr., W. C., Ed.; Springer-Verlag: New York, 1984; p 361.

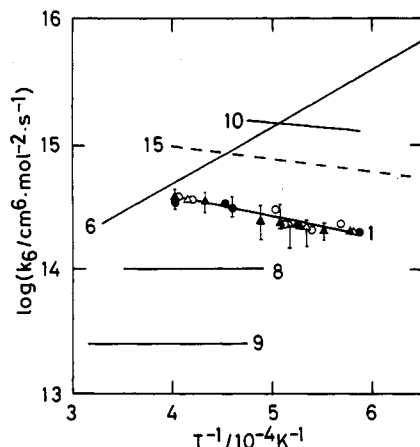


Figure 5. Arrhenius plots of the rate constants for $\text{CO} + \text{O} + \text{M} \rightarrow \text{CO}_2 + \text{M}$: 1, this work (\bullet , Δ , \blacktriangle , and \circ correspond to mixtures A, B, C, and D, respectively.); 15, Baulch et al.;¹⁵ 6, Lin et al.;⁶ 9, Dean et al.;⁹ 8, Zaslanko et al.;⁸ 10, Fujii et al.¹⁰

TABLE III: Reactions of Impurities and Rate Parameters^a

reaction	log A	B	E/kJ	ref
(8) $\text{H}_2\text{O} + \text{O} = \text{OH} + \text{OH}$	10.18	1.14	72.2	18
(9) $\text{CO} + \text{OH} = \text{CO}_2 + \text{H}$	6.64	1.5	-3.1	18
(10) $\text{N}_2\text{O} + \text{H} = \text{N}_2 + \text{OH}$	13.88	0	63.2	14
(11) $\text{O}_2 + \text{H} = \text{O} + \text{OH}$	17.08	-0.91	69.1	18
(12) $\text{CH}_4 + \text{O} = \text{CH}_3 + \text{OH}$	7.08	2.1	31.9	18
(13) $\text{CH}_3 + \text{O} = \text{CH}_2\text{O} + \text{H}$	13.85	0	0	18
(14) $\text{CH}_2\text{O} + \text{O} = \text{CHO} + \text{OH}$	13.54	0	14.7	18
(15) $\text{CHO} + \text{O} = \text{CO} + \text{OH}$	13.48	0	0	18

^a $k = AT^B \exp(-E/RT)$ (in units of $\text{cm}^3 \cdot \text{mol}^{-1}$ and s^{-1}).

k_1 and k_6 thus obtained are listed with the experimental conditions in Table II and Arrhenius plots of k_1 and k_6 are shown in Figure 4 and 5, respectively. The values of k_1 agreed well with those obtained in the previous work,¹⁰ and the effects of contaminant on the rate of reaction 1 was found to be small. However, the values of k_6 became about one order lower than the previous values.¹⁰ The difference is considered to originate from the impurities of He.

For CO_2 formation from CO with O or N_2O , it has been shown that small amounts of impurities such as organic compounds and water drastically affect the rate.^{8,9} Although small amounts of H_2O and O_2 are contained in the CO and N_2O used, the amounts in the mixtures do not exceed 20 and 100 ppm, respectively. The influence of the impurities was checked by a computer simulation using the scheme in Table II, with the addition of reactions 8–11 shown in Table III. At the maximum impurity level, the acceleration of CO_2 formation did not exceed 1% in the initial stage of reaction within about 200 μs . This result was supported by the experimental data shown in Figures 4 and 5; though the contents of CO and N_2O in the mixtures were changed from 2 to 5%, respectively, no systematic differences are observed in the figures.

The possibility that hydrocarbon impurities originating from the pump oil affects the CO_2 formation rate and that the effect predominates over reaction 1 was suggested.¹⁷ In order to check the effect of hydrocarbon impurities, numerical calculations by the following three models using reactions 1–7 and with the addition of reactions 8–14 shown in Table III were carried out for mixtures containing CH_4 (30 ppm): model A, reactions 1–7, the scheme of this work; model B, reactions 2–15, excluding reaction 1; model C, reactions 1–15. Typical results of the calculation are shown in Figure 6, together with the experimental results. From

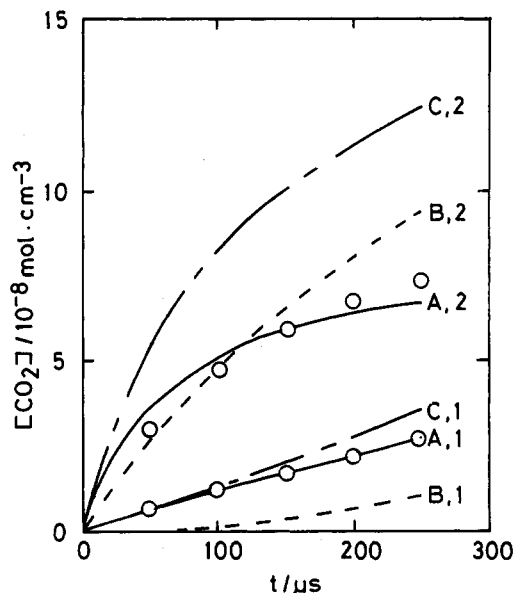


Figure 6. Comparison of the CO_2 concentration profiles calculated by the three models and those obtained by the experiment: (A, B, and C) from model A, B, and C, respectively; (\circ) from experiment; 1, $\text{CO}/\text{N}_2\text{O} = 5/5$, $T_0 = 1500$ K, $p_0 = 3.02$ atm; 2, $\text{CO}/\text{N}_2\text{O} = 5/5$, $T_0 = 2000$ K, $p_0 = 2.89$ atm.

the figure it is shown that, (1) at lower temperatures, the effect of the reaction of CH_4 (model C) does not become important at the initial stage of reaction, and when reaction 1 is excluded (model B), the rate of CO_2 formation becomes very slow. From the comparison, it is confirmed that reaction 1 is very important. (2) At higher temperatures, effect of the impurity is very large, and the calculated profiles B and C are very different from the experimental results. Here, the simulation is based upon the assumption that 30 ppm of CH_4 is present. However, the presence of impurities such as CH_4 is not considered in the present experiment, because an oil diffusion pump was used with a water-cooled baffle and a liquid N_2 cold trap, and the oil back streaming rate was less than 10^{-8} $\text{mg} \cdot \text{cm}^{-2} \cdot \text{min}^{-1}$ according to the manufacturer's measurement. From the above-described discussion, the rate constants obtained in the present work are not considered to have been affected by impurities.

The rate expression

$$k_1 = 9.8 \times 10^{10} \exp(-73 \text{ kJ}/RT) \text{ cm}^3 \cdot \text{mol}^{-1} \cdot \text{s}^{-1} \quad (1350\text{--}2500 \text{ K})$$

obtained from the Arrhenius plot in Figure 4 is very different from that obtained by other researchers. The data obtained by the single-pulse shock wave technique^{6,7} have some substantial errors which are much larger than those obtained by the conventional shock tube technique. For the data obtained mainly on CO-rich mixtures ($\text{CO} > 90\%$),^{5,8} the effect of the vibrational relaxation time on the rate measurement was not taken into account. The preexponential factor for k_1 obtained by us is very close to that obtained by Lin and Bauer⁶ and Milks and Matula.⁷ On the other hand, our activation energy 73 kJ is very close to that obtained by Milks and Matula,⁷ but much smaller than that obtained by Lin and Bauer.⁶ When compared with the exothermicity of reaction 1, $\Delta H_R = -365$ kJ,^{6,7} the lower value of the activation energy seems more acceptable.

The Arrhenius plot of the rate constant k_6 in Figure 5 is expressed by the equation

$$k_6 = 1.6 \times 10^{15} \exp(-30 \text{ kJ}/RT) \text{ cm}^6 \cdot \text{mol}^{-2} \cdot \text{s}^{-1} \quad (1700\text{--}2500 \text{ K})$$

The values of k_6 are smaller than those obtained in the author's previous work¹⁰ and by Lin and Bauer. The difference may be due to the effect of impurities on the rate measurements. The lower values by Dean and Steiner⁹ and by Zaslanko et al.⁸ may be due to the slow vibrational relaxation of CO-Ar and CO-CO .

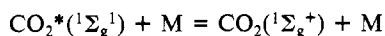
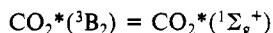
(15) Baulch, D. L.; Drysdale, D. D.; Duxbury, J.; Grant, S. In *Evaluated Kinetic Data for High Temperature Reactions*, Vol. 3; Butterworths: London, 1976; p 275.

(16) Fujii, N.; Sato, H.; Fujimoto, S.; Miyama, H. *Bull. Chem. Soc. Jpn.* **1984**, *57*, 277.

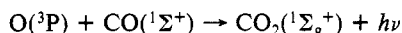
(17) Gardiner, Jr., W. C., private communication.

As shown in Figure 5, our present plot is rather similar to that of Baulch et al.¹⁵

Lin and Bauer⁶ obtained $k_6 = 2.8 \times 10^{12} \exp(99.6 \text{ kJ}) \text{ cm}^6 \text{ mol}^{-2} \text{ s}^{-1}$. In order to explain the negative activation energy, they proposed the following mechanism for the reaction:



Here, $\text{CO}_2^*(^3\text{B}_2)$ and $\text{CO}_2^*(^1\Sigma_g^+)$ represent vibrationally excited CO_2 in the $^3\text{B}_2$ and $^1\Sigma_g^+$ states, respectively. Further, they assumed that the rate-determining step is a transition between the $^3\text{B}_2$ state and the $^1\Sigma_g^+$ state and calculated that the crossing point between the $^3\text{B}_2$ and $^1\Sigma_g^+$ states is 31.4 kJ/mol below the $^3\text{B}_2$ dissociation limit. On the other hand, Clyne and Thrush¹⁹ studied the reaction



(18) Warnatz, J. In *Combustion Chemistry*, Gardiner, Jr., W. C., Ed.; Springer-Verlag: New York, 1984; p 197.

and found that the reaction is third order with a positive activation energy of 15.5 kJ. They claimed that the rate of CO_2 formation is not limited by spin change but by an energy barrier in the $^3\text{B}_2$ CO_2 potential curve which correlates with $\text{O}(^3\text{P}) + \text{CO}(^1\Sigma^+)$. They concluded that crossing from the $^3\text{B}_2$ state to the $^1\text{B}_2$, from which emission occurs, is rapid compared to the rate of barrier crossing. Later, Slanger et al.²⁰ obtained $k_6 = 2.3 \times 10^{15} \exp(-18.2 \text{ kJ}/RT) \text{ cm}^6 \text{ mol}^{-2} \text{ s}^{-1}$ over the temperature range 250–370 K, which was recommended by Baulch et al.¹⁵ They supported the above-described claim of Clyne and Thrush and calculated that there is a different mechanism taking place at the higher temperatures used in Lin and Bauer than that at the lower temperatures, if the shock tube experiment does not suffer from impurity problems.

The value of k_6 obtained by us supports the conclusions of Clyne and Thrush and Slanger et al. and indicates that reaction 6 proceeds via the same mechanism at both higher and lower temperatures.

(19) Clyne, M. A. A.; Thrush, B. A. *Proc. R. Soc. (London) Ser. A* **1962**, *A269*, 404.

(20) Slanger, T. G.; Wood, B. J.; Black, G. J. *Chem. Phys.* **1972**, *57*, 233.

High-Temperature Pyrolysis of Toluene

K. M. Pamidimukkala, R. D. Kern,

Department of Chemistry, University of New Orleans, New Orleans, Louisiana 70148

M. R. Patel, H. C. Wei, and J. H. Kiefer*

Department of Chemical Engineering, University of Illinois at Chicago, Chicago, Illinois 60680

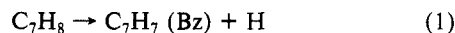
(Received: August 5, 1986; In Final Form: November 10, 1986)

The thermal decomposition of toluene has been investigated by two independent shock tube techniques: time-of-flight (TOF) mass spectrometry and laser-schlieren densitometry. These studies cover the temperature range 1550–2200 K for pressures 0.2–0.5 atm. C_2H_2 , C_4H_2 , CH_4 , and C_7H_7 were identified as major species along with lesser amounts of C_2H_4 , C_6H_2 , and C_6H_6 . The laser-schlieren profiles require a dominance by CC scission to phenyl and methyl with a rate constant $\log k \text{ (s}^{-1}\text{)} = 12.95 - 72.6 \text{ (kcal)}/2.3RT$ for 1600–2100 K and 0.5 atm. Such dominance is also required to produce the methane seen in the TOF spectra. A mechanism is proposed which provides an excellent description of density gradient and major species concentration profiles over this range.

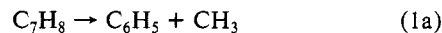
Introduction

Nearly all of the complications encountered in unimolecular decay kinetics occur in the decomposition of toluene: (a) the possibility of more than one dissociation channel, (b) an important contribution by recombination and other secondary processes, (c) falloff effects in both primary and secondary unimolecular processes, (d) discrepancies in the measured rate constants for key reactions, and (e) some uncertainty in the thermodynamic properties of important species.

Despite the above problems, toluene pyrolysis has generated much interest, undoubtedly motivated by toluene's popularity as a radical scavenger.¹ Here we are concerned with the pyrolysis kinetics at high temperatures ($T > 1000 \text{ }^\circ\text{C}$), and the very extensive lower temperature literature will not be generally considered (see Smith^{2,3} for a listing). We are particularly interested in the possible contribution of C–C bond scission to the dissociation. Following Szwarc's original work,⁴ this dissociation is usually taken to be confined to



(Bz denotes benzyl radical), but many workers (see Smith^{2,3}) have suggested the C–C scission



also runs in parallel.

There is no doubt that (1a) must occur; the issue is merely to what extent and under what conditions. Since the bond dissociation energies (BDE's) for (1) and (1a) differ by 15 kcal/mol (see below), the prejudice favoring reaction 1 is understandable. However, it is a common observation that separation into large radicals is accompanied by large A factors, exceeding 10^{17} s^{-1} in some instances, whereas that of (1) is probably little more than 10^{15} s^{-1} .⁵ On this rough basis, one might expect near equality of the high-pressure rates when the temperature reaches 1600 K.

The toluene pyrolysis is of course a chain reaction, as has been known and undisputed since the early work of Szwarc.⁴ Nevertheless, at high temperatures the product distribution can be

(1) Szwarc, M. *Chem. Rev.* **1950**, *47*, 75.

(2) Smith, R. D. *Combust. Flame* **1979**, *35*, 179.

(3) Smith, R. D. *J. Phys. Chem.* **1979**, *83*, 1553.

(4) Szwarc, M. *J. Chem. Phys.* **1948**, *16*, 128.

(5) Benson, S. W.; O'Neal, H. E. "Kinetic Data on Gas Phase Unimolecular Reactions"; *Natl. Stand. Ref. Data Ser. (U.S., Natl. Bur. Stand.)* **1970**, No. 21.